ORIGINAL ARTICLE

MiR-29a-3p Inhibits Proliferation and Osteogenic Differentiation of Human Bone Marrow Mesenchymal Stem Cells via Targeting FOXO3 and Repressing Wnt/β-Catenin Signaling in Steroid-Associated Osteonecrosis

Changgeng Wang, Minghui Zhu, Demeng Yang, Xinyuan Hu, Xinyuan Wen, Aimei Liu

Department of Emergency and Trauma Surgery, People's Hospital of Pingxiang, Pingxiang, China

Background and Objectives: This study was to investigate the role of microRNA-29a-3p (miR-29a-3p) in human bone marrow mesenchymal stem cells (hBMSCs), and its relationship with steroid-associated osteonecrosis.
Methods and Results: The online tool GEO2R was used to screen out the differentially expressed genes (DEGs) in GSE123568 dataset. Quantitative real time-polymerase chain reaction (qRT-PCR) was performed to detect the expression of miR-29a-3p, forkhead box O3 (FOXO3), alkaline phosphatase (ALP), bone gamma-carboxyglutamate protein (OCN) and RUNX family transcription factor 2 (Runx2) in the hBMSCs isolated from the patients with steroid-associated osteonecrosis. CCK-8 assay was executed to measure cell viability; western blot assay was utilized to detect FOXO3, ALP, Runx2, OCN and β-catenin expression. Cell apoptosis and cell cycle were detected by flow cytometry. Immunofluorescence assay was used to detect the sub-cellular localization of β-catenin. Bioinformatics analysis and luciferase reporter gene assay were performed to confirm whether miR-29a-3p can combine with FOXO3 3'UTR. MiR-29a-3p was markedly up-regulated in the hBMSCs of patients with steroid-associated osteonecrosis, while FOXO3 mRNA was significantly down-regulated. Transfection of miR-29a-3p mimics significantly inhibited the hBMSCs' proliferation, osteogenic differentiation markers' expressions, including ALP, Runx2, OCN, and repressed the ALP activity, as well as promoted cell apoptosis and cell-cycle arrest. FOXO3 was identified as a target gene of miR-29a-3p, and miR-29a-3p can inhibit the expression of FOXO3 and β-catenin, and inhibition of miR-29a-3p promoted translocation of β-catenin to the nucleus.
Conclusions: MiR-29a-3p can modulate FOXO3 expression and Wnt/β-catenin signaling to inhibit viability and osteogenic differentiation of hBMSCs, thereby promoting the development of steroid-associated osteonecrosis.

Keywords: Steroid-associated osteonecrosis, miR-29a-3p, FOXO3, Wnt/β-catenin

Introduction

Osteonecrosis of the femoral head (ONFH) is common bone disease in clinical practice (1). The use of excessive glucocorticoid is a risk factor for non-traumatic osteonecrosis of the femoral head, resulting in steroid-associated osteonecrosis (SAON) (2). Currently, the detailed mechanisms underlying ONFH remain unclear.

Bone marrow mesenchymal stem cells (BM-MSCs) are a class of multipotent stem cells located in the mesoderm. Under different conditions, human bone marrow mesen-

chymal stem cells (hBMSCs) can differentiate into different cells, such as adipocytes, osteoblasts and chondrocytes (3). Osteogenic differentiation is a highly ordered process, of which Runt-related transcription factor 2 (RUNX2) is a vital transcription factor in the process of osteogenesis, and during this process, alkaline phosphatase (ALP) expression and activity is increased; also, osteogenesis is related to the mineralization-related gene osteocalcin (OCN) (4). Reportedly, the adverse impacts of glucocorticoid on the viability of hBMSCs and osteogenic differentiation are one of the major factors in the failure of bone repair and regeneration (5).

MicroRNAs (miRNAs), short non-coding transcripts of approximately $18 \sim 25$ nt in length, can negatively regulate the target genes' expression via binding to the 3' untranslated region (3'UTR) of target genes (6). MiRNAs play crucial roles in the progression of ONFH (7-10). For example, miR-23b-3p played a protective role in steroid-induced ONFH by suppressing ZNF667 expression (8); miR-145 plays a role in the progression of steroid-induced ONFH by targeting the OPG/RANK/RANKL signaling pathway (9); by targeting DKK1, miR-217 promotes proliferation and osteogenic differentiation of BMSCs in steroid-associated osteonecrosis (10). MiR-29a-3p, reportedly, is a pivotal regulator in cancer biology. Specifically, miR-29a-3p dysregulation takes part in the progression of certain cancers, such as osteosarcoma (11), breast cancer (12), endometrial cancer (13), hepatocellular carcinoma (14). Instead, the role of miR-29a-3p in ONFH and SAON is unknown.

The forkhead box O (FOXO) transcription factor family members regulate cell cycle progression, DNA repair and senescence (15). It is reported that FOXO3 is involved in osteogenic differentiation of mesenchymal stem cells (16). The present study report that miR-29a-3p can regulate the hMSCs growth and osteogenic differentiation by regulating FOXO3. Our study may shed new light on SAON therapy.

Materials and Methods

Patient recruitment

The work was endorsed by the Ethics Committee of People's Hospital of Pingxiang. 15 patients were diagnosed with glucocorticoid-related ONFH were recruited from 2016 to 2020. In addition, 13 individuals with femoral neck fractures due to trauma were recruited as controls. These patients received artificial femoral head replacement, and the femoral head tissues were obtained. The characteristics of participants were shown in Table 1.

Informed consent was accordingly obtained from all patients prior to surgery. Bone marrow samples were collected intraoperatively and placed in heparin anticoagulant tubes.

Cell culture

To isolate the hBMSCs, serum-free minimum essential medium α (α-MEM) containing 100 UI/ml penicillin and 0.1 μg/ml streptomycin was mixed with the bone marrow samples. Bone marrow samples were centrifuged at room temperature, with the fat layer discarded. The cells were subsequently resuspended in α-MEM and Percoll was slowly loaded. The mixture was centrifuged for 30 min, and the intermediate monocyte layer was aspirated and discarded. After rinsing twice with phosphate buffer saline (PBS), the cells were resuspended in α-MEM with 10% fetal bovine serum, and routinely cultured. Subsequent to adjusting the cell concentration to 1×10^6 /ml, the cells were inoculated in culture flasks until reached 80% confluence. Osteogenic differentiation was subsequently induced with α-MEM containing 10% fetal bovine serum, 0.1 μmol/l dexamethasone, 10 mmol/l β-glycerophosphate, and 50 mg/l vitamin C. In addition, we added 40 μM XAV939 (Selleckchem, Houston, Texas, USA) to the medium and examined the impacts of the Wnt/β-catenin pathway on cell growth and osteogenic differentiation.

Cell transfection

MiR-29a-3p mimics, miR-29a-3p inhibitors and their control miR-NC, FOXO3 overexpression plasmid and empty plasmid were available from Genomeditech (Shanghai, China). The oligonucleotides and plasmids were transfected into hBMSCs by Lipofectamine 3000 (Invitrogen, Carlsbad, CA, USA) according to the manufacturer's instruction. 48 h after the transfection, the cells were harvested for the subsequent experiments.

Quantitative real time polymerase chain reaction (qRT-PCR)

Total RNA extracted from hBMSCs by TRIzol kit (Invitrogen, Carlsbad, CA, USA) was reversely transcribed into cDNA by a Transcriptor First Strand cDNA Synthesis

Table 1. The characteristics of participants

	SAON (n=15)	Control (n=13)
Age (mean±SD)	55.1±6.9	60.2±7.5
Gender (male/female)	4/11	8/5
BMI (kg/m^2)	25.8±4.2	24.9±5.8

kit (Roche, Basel, Switzerland), and the SYBR Green PCR Master Mix (Qiagen, Valencia, CA, USA) was mixed with cDNA and primers to perform qRT-PCR. The relative RNA expression was calculated by $2^{-\Delta\Delta Ct}$ method. The primer sequences are: miR-29a-3p: 5'-CTGGTGTCGTGG AATTCAGTTGA-3' (Forward), 5'-CCTGGCTCCTCACT TGGC-3' (Reverse); miR-23a-3p: 5'-CGGATCACATTGC CAGGG-3' (Forward), 5'-CAGTGCGTGTCGTGGAGT-3' (Reverse); miR-96-5p: 5'-ATGCTTTCTCAACTTGTTGG-3'(Forward), 5'-TCACCGCTCTTGGCCGTCACA-3' (Reverse); miR-9-5p: 5'-GTGCAGGGTCCGAGGT-3' (Forward), 5'-GCGCTCTTTGGTTATCTAGC-3' (Reverse); miR-182-5p: 5'-CCCAACTGTATGGTTT-3'(Forward), 5'-CGGA TGGCCCAACGG-3'(Reverse). FOXO3: 5'-CAGCCGAGG AAATGTTCGTC-3' (Forward), 5'-AGAGTGAGCCGTTT GTCCG-3' (Forward); U6:5'-GCTTCGGCAATACTAAAA T-3' (Reverse), 5'-CGCTTCACGAATTTGCGTCATGT-3' (Reverse); GAPDH: 5'-GGAGCGAGATCCCTCCAAAAT-3' (Forward), 5'-GGCTGTCATACTTCTAATGG-3' (Reverse).

Cell viability measurement

The viability of hBMSCs was detected with Cell Counting Kit-8 (CCK-8) (Yeasen, Shanghai, China). The transfected cells were seeded at 3×10^3 cells per well into a 96-well plate and cultured, followed by addition of 10 μl CCK-8 solution at 0 h, 24th h, 48th h and 72nd h and incubation for 2 h at 37℃, and ultimately the absorbance value at 450 nm wavelength was measured by a microplate reader (Thermo-Fisher Scientific, Waltham, MA, USA).

ALP activity detection

Transfected hBMSCs were cultured in 6-well plates for 48 h. Subsequently, hBMSCs were rinsed three times with PBS, and next, the ALP activity of hBMSCs was detected by the ALP activity detection kit (Sigma-Aldrich, St. Louis, MO, USA).

Western blot assay

Total proteins in the hBMSCs were extracted by radioimmunoprecipitation assay (RIPA) lysis buffer (Beyotime, Shanghai, China) on ice, and subsequently quantified by the bicinchoninic acid (BCA) protein assay. Then the loading buffer was added into the protein samples, and heated in boiling water for 10 min. Next, the same amount of protein samples in each group were respectively separated by sodium dodecyl sulfate-polyacrylamide gel electrophoresis and transferred to the polyvinylidene fluoride membrane, which was firstly incubated overnight at 4℃ with primary antibodies (anti-FOXO3: ab109629, Abcam Cambridge, UK; anti-ALP: ab224335, Abcam secondary

Cambridge, UK; anti-Runx2: ab192256, Abcam Cambridge, UK; anti-OCN: ab133612, Abcam Cambridge, UK; anti-GAPDH: ab9485, Abcam, Cambridge, UK), and secondly with horseradish peroxidase-labeled secondary antibody (ab6721, Abcam Inc., Cambridge, UK). Finally, the protein bands were shown by an ECL detection reagent (Beyotime, Shanghai, China).

Immunofluorescence assay

For immunofluorescence analysis, cells were seeded in the 12-well plates, then fixed with 4% formaldehyde for 30 min and treated with 0.5% Triton X-100 for 20 min. Subsequently, the cells were incubated with anti-β-catenin antibody (#8480, Cell Signaling Technology, Shanghai, China) at room temperature for 1 h. Then incubated with the corresponding secondary antibody (#4414, Cell Signaling Technology, Shanghai, China) in the darkness at room temperature for 1 h. The cell nuclei were then stained with DAPI. Images were captured by a fluorescent microscope.

Flow cytometry

For cell cycle assay, the cells were washed with PBS and fixed with cold ethanol for 2 h. Then the cells were stained with propidium iodide (PI) staining solution for 30 min at room temperature in the dark. Then the cells were detected by flow cytometry and the data were analyzed by the FCS 4 Express Flow Cytometry Software (De Novo Software, Glendale, CA, USA). For cell apoptosis assay, the Annexin V-fluorescein isothiocyanate (FITC)/PI Apoptosis Detection kit (Beyotime, shanghai, China) was used. Briefly, the cells were harvested and resupended in binding buffer, and stained with 5 μl of Annexin V-FITC staining solution for 15 min at room temperature in the dark, and then stained with 5 μl of PI staining solution for 5 min at room temperature in the dark. Then the cells were detected by flow cytometry and the data were analyzed by the FCS 4 Express Flow Cytometry Software (De Novo Software, Glendale, CA, USA).

Luciferase reporter gene assay

FOXO3 3'UTR sequence containing a binding site with miR-29a-3p was subsequently amplified, and the PCR product was generally cloned into pGL3 Basic reporter vectors (Promega, Madison, WI, USA) to generate the wild type (WT) FOXO3-WT luciferase reporter vector. FOXO3 3'UTR complementary sequence was subsequently mutated and inserted into the reporter vector to generate mutant type (MUT) FOXO3-MUT luciferase reporter vector. Then, the above luciferase reporter plasmids were re-

spectively transfected into 293T cells with miR-NC and miR-29a-3p mimics. 24 h after transfection, the luciferase activity was evaluated by the Dual-Luciferase Reporter Assay System (Promega, Madison, WI, USA). The relative luciferase activity=(Firefly luciferase activity/Renilla luciferase activity)×100%.

Statistical analysis

Statistical analysis was performed with Statistical Product and Service Solutions (SPSS) 22.0 software (IBM, Armonk, NY, USA), and all experimental results were expressed as mean±standard deviation. Student t-test was subsequently executed to compare the differences between two groups, and one-way ANOVA test was adopted to compare the differences among three groups. Correlation analysis was accordingly performed by Pearson's correlation analysis, and statistically, $p < 0.05$ is meaningful.

Results

miR-29a-3p is greatly raised in patients with SAON and significantly downregulated in FOXO3

To explore the differentially expressed genes (DEGs) in the serum of SAON patients, we downloaded microarray gene profiling dataset (GSE123568) which contains 30 SAON patients and 10 non-SAON individuals from the Gene Expression Omnibus (GEO) for bioinformatics analysis. The mRNAs with p-value < 0.05 and $|\log_2 FC| \geq$ 1.0 were identified as the DEGs. A total of 1402 DEGs were selected (Fig. 1A). Then, the down-regulated DEGs were analyzed by Gene Ontology (GO) and Kyoto Encyclopedia of Genes and Genomes (KEGG) enrichment analysis, and GO analysis hinted that the DEGs were enriched in the oxidation-reduction process, protein phosphorylation, negative regulation of transcription from RNA polymerase II promoter, cell proliferation, protein ubiquitination and negative regulation of apoptotic process (Fig. 1B). KEGG pathway analysis indicated that the DEGs were enriched in FOXO signaling pathway (Fig. 1C). Previous studies have revealed that overexpression of a FOXO3 transgene in mature osteoblasts decreased oxidative stress and osteoblast apoptosis and increased the rate of bone formation (17), then FOXO3 was selected in our research, and notably it was also down-regulated in the SAON samples in GSE123568 (Fig. 1A). Next, we identified 5 common miRNAs which could target FOXO3 by searching miRDB, miRTarase, miRwalk and Targetscan databases. qRT-PCR revealed that FOXO3 mRNA expression was relatively lower in SAON group than that in the control group (Fig. 1E). miR-29a-3p and miR-23a-3p

were expressed at higher levels in the hBMSCs isolated from 15 SAON patients than that from the 13 control subjects, however, the expression of miR-96-5p, miR-9-5p and miR-182-5p between two groups have no significant difference (Fig. 1E and Supplementary Fig. S1A~D). Correlation analysis confirmed that miR-29a-3p expression and FOXO3 mRNA expression in the samples from SAON patients were negatively correlated, and there is no connection between miR-23a-3p and FOXO3 mRNA expression (Fig. 1F and Supplementary Fig. S1E). The above results suggest that miR-29a-3p and FOXO3 may be implicated in SAON progression.

miR-29a-3p restrains hBMSCs' viability, cell cycle progression and osteogenic differentiation

To identify the role of miR-29a-3p in the proliferation, cell cycle and osteogenic differentiation of hBMSCs, we transfected miR-29a-3p mimics, miR-29a-3p inhibitors and control miR-NC into hBMSCs and successfully constructed miR-29a-3p overexpression and low expression models (Fig. 2A). We examined Runx2, ALP and OCN expression after the induction of osteogenic differentiation of hBMSCs, and observed that miR-29a-3p mimics remarkably inhibited the expression of Runx2, ALP and OCN, as well as ALP activity, while the transfection of miR-29a-3p inhibitors functioned oppositely (Fig. 2B~F). Flow cytometry revealed that overexpression of miR-29a-3p induced apoptosis of hBMSCs, and miR-29a-3p inhibitor showed the opposite effect (Fig. 2G and 2H). CCK-8 assay revealed that the transfection of miR-29a-3p mimics dramatically restrained the viability of hBMSCs, while miR-29a-3p inhibitors promoted the viability of hBMSCs (Fig. 2I). Cell cycle analysis revealed that overexpression of miR-29a-3p induced cell-cycle arrest at G1-G0 phase, and miR-29a-3p inhibitor showed the opposite effect (Fig. 2J and 2K). These findings confirmed that miR-29a-3p restrains hBMSCs growth and osteogenic differentiation, as well as induces cell apoptosis and cell-cycle arrest.

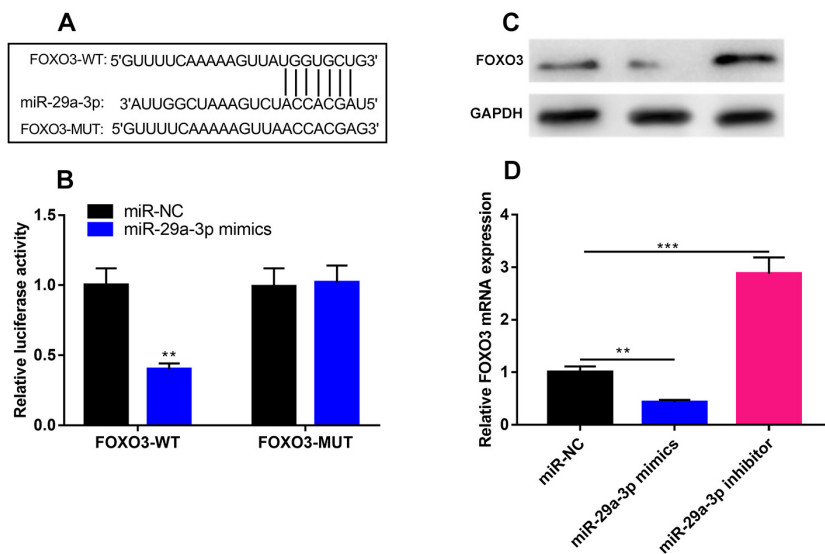### In hBMSCs, miR-29a-3p can negatively regulates FOXO3 expression

FOXO3 3'UTR contained the potential binding site complementary to miR-29a-3p (Fig. 3A). To further confirm their specific binding relationship, a dual-luciferase reporter assay was performed, and it was found that the transfection of miR-29a-3p mimics greatly repressed the luciferase activity of FOXO3-WT-containing luciferase reporter plasmids but had no impacts on that of FOXO3-MUT-containing luciferase reporter plasmids (Fig. 3B). qRT-PCR and western blot showed that the transfection
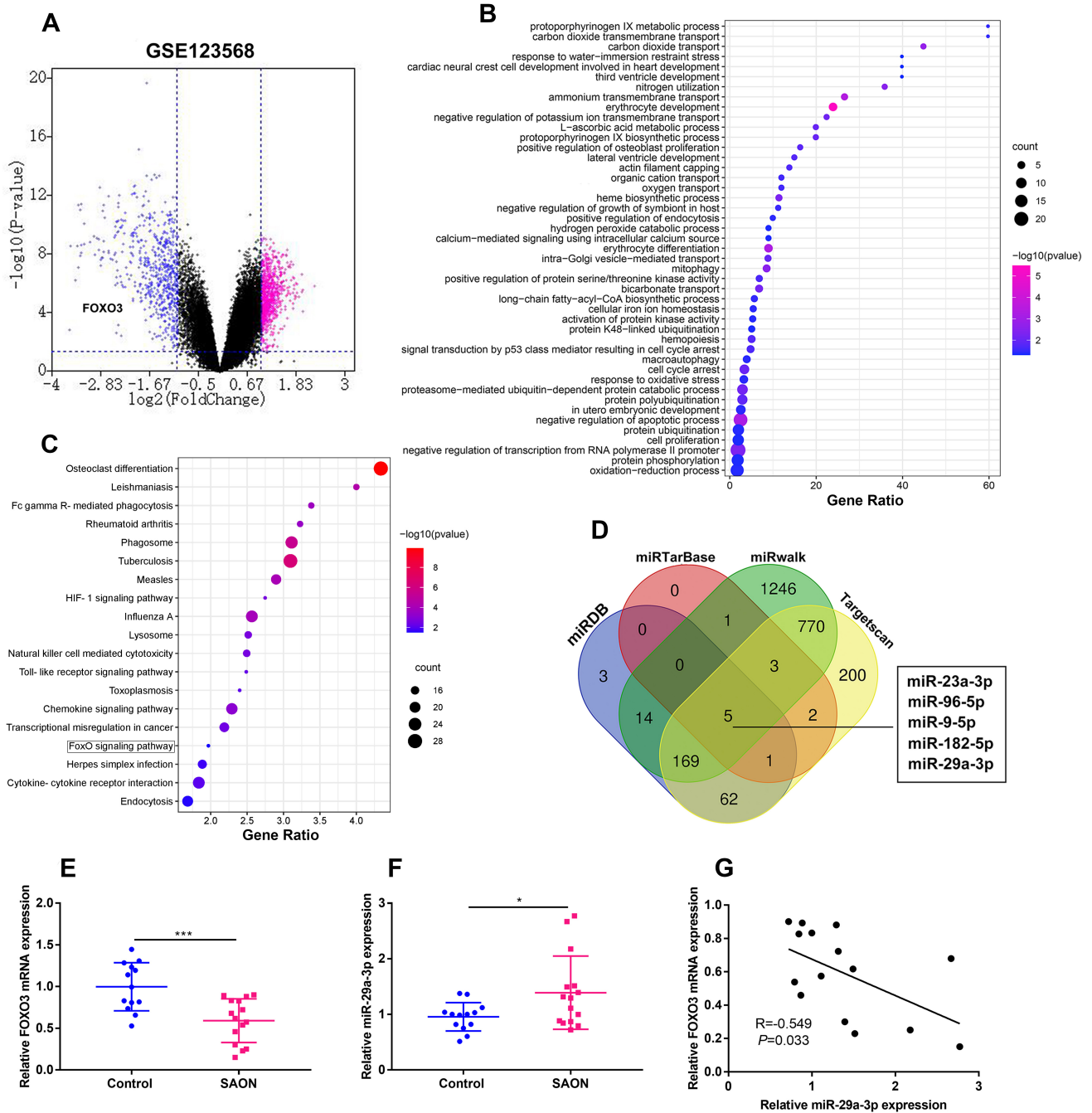
Fig. 1. miR-29a-3p is significantly up-regulated and FOXO3 is significantly down-regulated in the hBMSCs isolated from SAON patients. (A) The volcano plot was used to show the DEGs in 30 SAON patients and 10 non-SAON individuals from the GSE123568. Genes whose expressions were significantly increased were marked in red, and those whose expressions were significantly decreased were marked in blue. (B, C) GO and KEGG enrichment analysis of the down-regulated DEGs in the GSE123568. (D) Venn diagram was used to screen the common miRNAs which could target FOXO3 among miRDB, miRTarase, miRwalk and Targetscan databases. (E) FOXO3 mRNA expression was detected by qRT-PCR in the hBMSCs from SAON patients and patients with fracture. (F) miR-29a-3p expression was measured by qRT-PCR in the hBMSCs from SAON patients and patients with fracture. (G) Correlation analysis of miR-29a-3p and FOXO3 mRNA in the hBMSCs from SAON patients. *p<0.05, ***p<0.001.
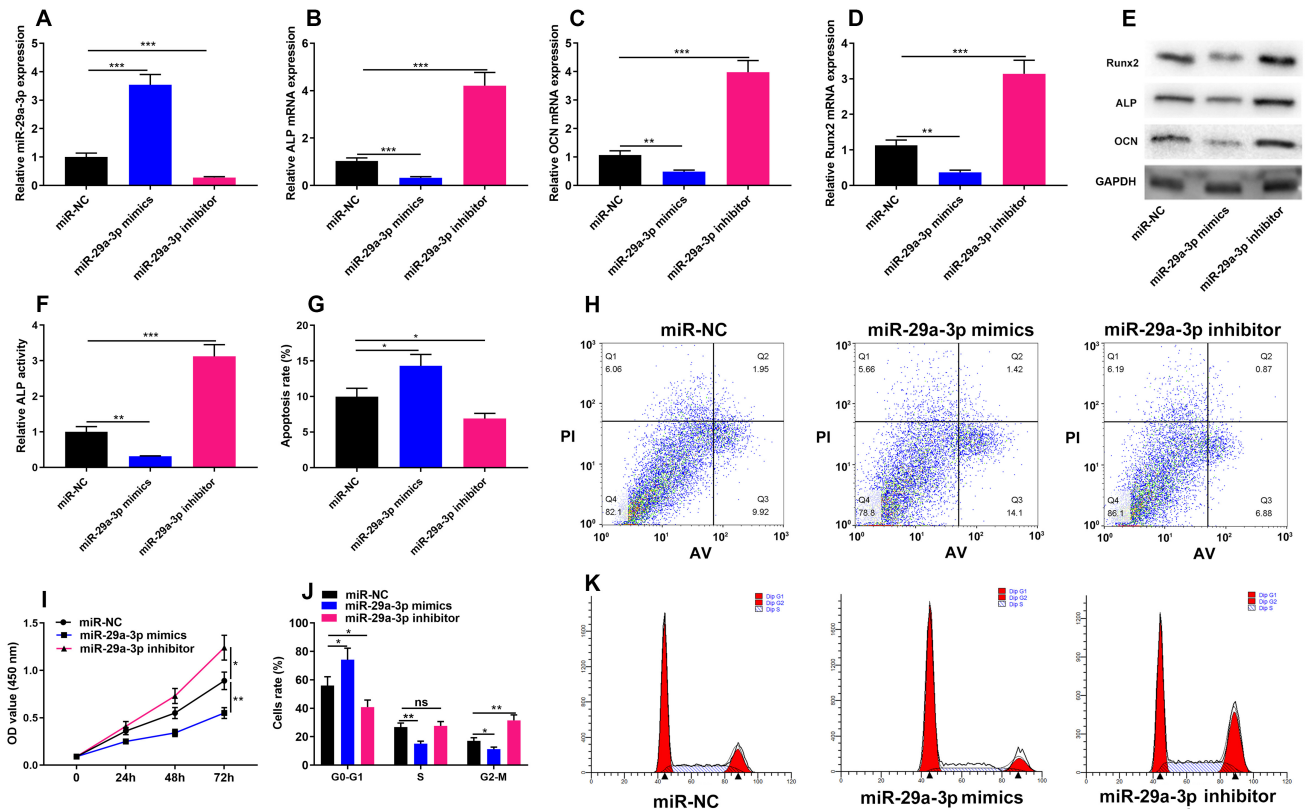
Fig. 2. miR-29a-3p inhibits cell proliferation and osteogenic differentiation of hBMSCs. (A) The expression of miR-29a-3p in hBMSCs transfected with miR-29a-3p mimics and miR-29a-3p inhibitors was detected by qRT-PCR. (B~E) qRT-PCR and Western blot assay was used to detect Runx2, ALP and OCN mRNA and protein expression, markers of osteogenic differentiation, in hBMSCs transfected with miR-29a-3p mimics or miR-29a-3p inhibitors. (F) The ALP activity of hBMSCs transfected with miR-29a-3p mimics or miR-29a-3p inhibitors was measured. (G, H) Flow cytometry was used to detect the apoptosis of hBMSCs transfected with miR-29a-3p mimics or miR-29a-3p inhibitors. (I) CCK-8 assay was used to detect the viability of hBMSCs transfected with miR-29a-3p mimics or miR-29a-3p inhibitors. (J, K) Flow cytometry was used to detect the cell cycle of hBMSCs transfected with miR-29a-3p mimics or miR-29a-3p inhibitors. *p<0.05, **p<0.01, ***p<0.001.

Fig. 3. In hBMSCs, miR-29a-3p negatively regulates the expression of FOXO3. (A) Bioinformatics analysis revealed that the FOXO3 3′UTR contained a potential binding site complementary to miR-29a-3p. (B) Dual-luciferase reporter gene assay confirmed that miR-29a-3p could directly bind to FOXO3 3′UTR. (C, D) qRT-PCR and western blot assays were performed to detect the expression of FOXO3 mRNA and protein in hBMSCs transfected with miR-29a-3p mimics or miR-29a-3p inhibitors. *p<0.01, **p<0.001.

of miR-29a-3p mimics significantly decreased FOXO3 expression compared with miR-NC, while miR-29a-3p inhibitors functioned oppositely (Fig. 3C and 3D). The above results confirmed that FOXO3 was a downstream target of miR-29a-3p in hBMSCs.

FOXO3 overexpression reverses the inhibitory effect of miR-29a-3p on cell viability and osteogenic differentiation of hBMSCs

Next, we co-transfected the FOXO3 overexpression plasmid and miR-29a-3p mimics into hBMSCs and found that FOXO3 overexpression plasmid partially counteracted the inhibitory impact of miR-29a-3p mimic on the expression of osteogenic differentiation markers, including Runx2, ALP and OCN (Fig. 4A~D), and the viability of hBMSCs (Fig. 4E), as well as the ALP activity (Fig. 4F). Additionally, FOXO3 overexpression significantly reversed the apoptosis (Fig. 4G) and cell-cycle arrest (Fig. 4H) of hBMSCs induced by miR-29a-3p overexpression. The above results implied that miR-29a-3p repressed hBMSCs' viability and osteogenic differentiation through FOXO3.

miR-29a-3p modulates hBMSC proliferation and osteogenic differentiation through Wnt/β-catenin signaling

Some previous studies report that miR-29a-3p can regulate the activity of Wnt/β-catenin signaling (18, 19), and considering Wnt/β-catenin is a crucial pathway to modulate the osteogenic differentiation of hBMSCs (20), it is also interesting to explore whether miR-29a-5p inhibited hBMSCs cell growth and osteogenic differentiation by regulating the Wnt/β-catenin signaling pathway. We detected β-catenin protein expression in hBMSCs transfected with miR-29a-3p inhibitors and miR-29a-3p mimics, and found that as against the miR-NC group, the transection of miR-29a-3p inhibitors significantly promoted β-catenin expression, while the transfection of miR-29a-3p mimics worked oppositely, and the immunofluorescence assay showed that transfection of miR-29a-3p inhibitor could promoted β-catenin nuclear translocation (Fig. 5A~C). Subsequently, XAV939, a specific inhibitor of Wnt/β-catenin signaling pathway was used to treat the cells, and the results showed that XAV939 could partially reverse the impact of miR-29a-3p inhibitors on the osteogenic differentiation (Fig. 5E~G), viability (Fig. 5H), ALP activity (Fig. 5I), apoptosis (Fig. 5J) and cell-cycle arrest (Fig. 5K) of hBMSCs. These data suggested that miR-29a-3p could also regulate the phenotypes of
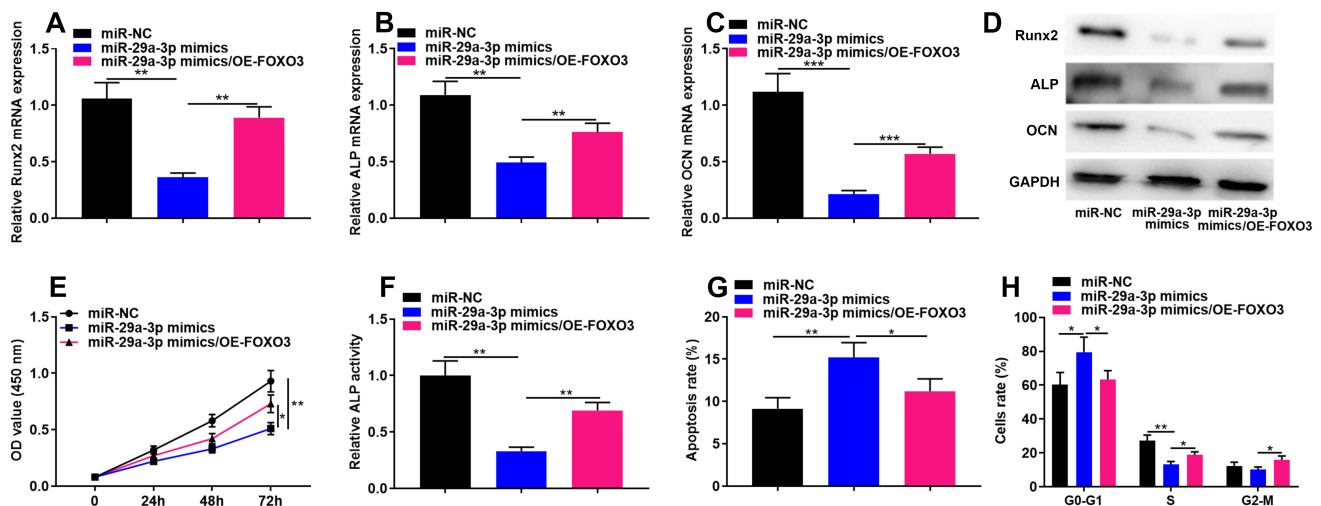
Fig. 4. FOXO3 overexpression plasmid reverses the inhibitory effect of miR-29a-3p on cell proliferation and osteogenic differentiation of hBMSCs. (A~D) qRT-PCR and Western blot assay was performed to detect Runx2, ALP and OCN mRNA and protein expression, markers of osteogenic differentiation, in hBMSCs co-transfected with miR-29a-3p mimics and FOXO3 overexpression plasmids. (E) CCK-8 assay was used to detect the viability of hBMSCs after co-transfection with miR-29a-3p mimics and FOXO3 overexpression plasmids. (F) ALP activity in hBMSCs was measured after co-transfection with miR-29a-3p mimics and FOXO3 overexpression plasmids. (G, H) Flow cytometry was used to detect cell apoptosis and cell cycle in hBMSCs transfected with miR-29a-3p mimics and FOXO3 overexpression plasmids. *p<0.05, **p<0.01.
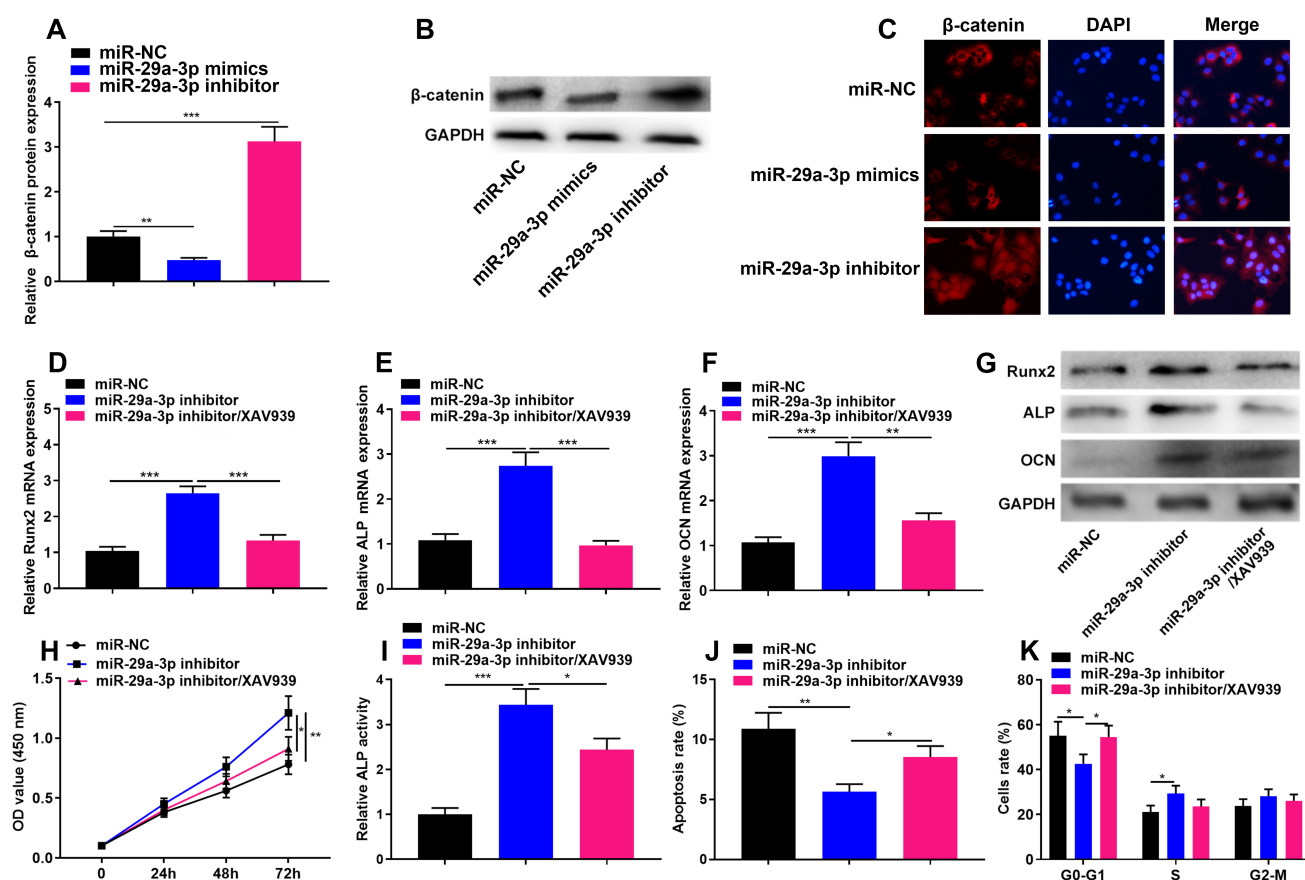
Fig. 5. miR-29a-3p regulates cell proliferation and osteogenic differentiation of hBMSCs through Wnt/β-catenin signaling. (A, B) Western blot assay was used to detect β-catenin protein expression in hBMSCs transfected with miR-29a-3p mimics or miR-29a-3p inhibitors. (C) Immunofluorescence assay was used to detect the subcellular expression of β-catenin. (D~G) qRT-PCR and Western blot assay was used to detect Runx2, ALP and OCN mRNA and protein expression, markers of osteogenic differentiation, in hBMSCs transfected with miR-29a-3p inhibitors and treated with XAV939. (H) CCK-8 assay was used to detect proliferation in hBMSCs transfected with miR-29a-3p inhibitors and treated with XAV939. (I) The ALP activity of hBMSCs transfected with miR-29a-3p inhibitors and treated with XAV939 was detected. (J, K) Flow cytometry was used to detect the apoptosis and cell cycle of hBMSCs transfected with miR-29a-3p inhibitors and treated with XAV939. *p<0.05, **p<0.01, **p<0.001.

hBMSCs via repressing Wnt/β-catenin signaling.

Discussion

The widespread use of glucocorticoids has led to an increased incidence of ONFH, instead, the underlying mechanisms involved in its pathogenesis are still indeterminate. It is well known that miRNAs act as post-transcriptional regulators and exert their biological functions by repressing the translation of target mRNAs. Reportedly, miRNAs regulate a variety of physiological and pathological processes. Besides, the aberrant expression of miRNAs may be associated with the pathogenesis of bone-related metabolic diseases, including ONFH (21). Many studies have reported that aberrant expression of miR-29a-3p is involved in the development of many

diseases. For example, in endometrial cancer, miR-29a-3p inhibits cell proliferation, migration and invasion by targeting VEGFA/CDC42/PAK1 signaling pathway (13). MiR-29a-3p suppressed the migration and proliferation of HeLa cells by directly targeting SNIP1 (22). Additionally, it is reported that miR-29a-3p can attenuate arthritis progression in mice with collagen-induced arthritis (23). Here we report that miR-29a-3p expression level was raised in the hBMSCs of SAON patients and it could inhibit the viability and osteogenic differentiation of hBMSCs, as well as induced cell apoptosis and cell cycle arrest. Our data suggest that inhibiting miR-29a-3p may be a promising strategy to treat the patients with SAON.

FOXO family transcription factors play important roles in many biological processes, such as cell proliferation, apoptosis and differentiation (24). Previous studies have

shown that FOXOs are involved in regulating osteogenic differentiation and maintaining skeletal homeostasis. Knockdown of FOXO1, FOXO3 and FOXO4 in mice results in increased bone oxidative stress, enhanced osteolast apoptosis and reduces osteoblast number, whereas overexpression of FOXO3 in osteoblasts inhibits oxidative stress, suppresses apoptosis and increases bone formation (17). Another study reports that, FOXO3, which is targeted by miR-223-3p, can increase the level of ALP and promoting osteogenic differentiation of hBMSCs by enhancing autophagy (25). Furthermore, FOXO3 induces autophagy and thereby reduces reactive oxygen species, which is resulted from the increased mitochondrial respiration during osteoblast differentiation in hBMSCs (16). These studies mentioned above support that FOXO3 is a protective factor for bone disease. Here we demonstrate that FOXO3 is significantly down-regulated in hBMSCs of patients with SAON; additionally, previous study revealed that FOXO3A as a direct target of miR-29a and is essential for the differentiation of mesenchymal stem cells (MSCs) into chondrocytes and cartilage/bone formation *in vivo* (26). Our result is similar with it, showing that FOXO3 is identified as the downstream target gene of miR-29a-5p, and miR-29a-5p represses the growth and osteogenic differentiation of hBMSCs via repressing FOXO3.

The Wnt/β-catenin pathway is an important regulatory pathway for osteogenesis. Previous studies report that Wnt/β-catenin signaling can increase the number of osteoblasts and facilitate bone formation (27). β-catenin induces osteoblast proliferation and reduces apoptosis by directly activating the expression of Runx2 (28). In addition, it has also been reported that in a rat model with steroid-associated ONFH, inhibition of the Wnt/β-catenin signaling pathway reduces the osteogenic capacity of BMSCs and enhances adipogenic capacity (29). It has been validated that miR-29a-3p can directly suppress the activity of Wnt/β-catenin pathway via targeting DVL2 and FZD4 in the BMSCs of a rat model (18). In this work, it was revealed that miR-29a-3p regulated hBMSCs' viability and osteogenic differentiation through Wnt/β-catenin signal pathway, and inhibiting Wnt/β-catenin pathway could partially reverse the promoting effect of miR-29a-3p inhibitors on hBMSCs cell growth and osteogenic differentiation. These data provide another explanation for the mechanisms by which miR-29a-3p participates in the pathogenesis of SAON.

On all accounts, this study confirms that miR-29a-3p restrains the viability and osteogenic differentiation of hBMSCs via targeting FOXO3 and suppressing Wnt/β-catenin signaling, which partly explains the mechanism of SAON pathogenesis, and provides clues for the treatment of this disease. In the following studies, *in vivo* model is needed to further validate our conclusion, and the detailed mechanism by which glucocorticoids repress miR-29a-3p expression in hBMSCs should be explored.

Potential Conflict of Interest

The authors declare that they have no competing interests.

Supplementary Materials

Supplementary data including one figure can be found with this article online at https://doi.org/10.15283/ijsc21147.

References

1. Bose VC, Baruah BD. Resurfacing arthroplasty of the hip for avascular necrosis of the femoral head: a minimum follow-up of four years. J Bone Joint Surg Br 2010;92:922-928
2. Yue J, Wan F, Zhang Q, Wen P, Cheng L, Li P, Guo W. Effect of glucocorticoids on miRNA expression spectrum of rat femoral head microcirculation endothelial cells. Gene 2018;651:126-133
3. Su P, Tian Y, Yang C, Ma X, Wang X, Pei J, Qian A. Mesenchymal stem cell migration during bone formation and bone diseases therapy. Int J Mol Sci 2018;19:2343
4. Park KR, Kim S, Cho M, Kang SW, Yun HM. Effects of PIN on osteoblast differentiation and matrix mineralization through Runt-related transcription factor. Int J Mol Sci 2020;21:9579
5. Deng S, Dai G, Chen S, Nie Z, Zhou J, Fang H, Peng H. Dexamethasone induces osteoblast apoptosis through ROS-PI3K/AKT/GSK3β signaling pathway. Biomed Pharmacother 2019;110:602-608
6. Beyer C, Zampetaki A, Lin NY, Kleyer A, Perricone C, Iagnocco A, Distler A, Langley SR, Gelse K, Sesselmann S, Lorenzini R, Niemeier A, Swoboda B, Distler JH, Santer P, Egger G, Willeit J, Mayr M, Schett G, Kiechl S. Signature of circulating microRNAs in osteoarthritis. Ann Rheum Dis 2015;74:e18
7. Wang J, Liu S, Li J, Zhao S, Yi Z. Roles for miRNAs in osteogenic differentiation of bone marrow mesenchymal stem cells. Stem Cell Res Ther 2019;10:197
8. Liu Y, Zong Y, Shan H, Lin Y, Xia W, Wang N, Zhou L, Gao Y, Ma X, Jiang C. MicroRNA-23b-3p participates in steroid-induced osteonecrosis of the femoral head by suppressing ZNF667 expression. Steroids 2020;163:108709
9. Zhao JJ, Wu ZF, Wang L, Feng DH, Cheng L. MicroRNA-145 mediates steroid-induced necrosis of the femoral head by targeting the OPG/RANK/RANKL signaling pathway. PLoS One 2016;11:e0159805
10. Dai Z, Jin Y, Zheng J, Liu K, Zhao J, Zhang S, Wu F, Sun Z. MiR-217 promotes cell proliferation and osteogenic differentiation of BMSCs by targeting DKK1 in ste-

roid-associated osteonecrosis. Biomed Pharmacother 2019; 109:1112-1119

11. Jin H, Wang H, Jin X, Wang W. Long non-coding RNA H19 regulates LASP1 expression in osteosarcoma by competitively binding to miR-29a-3p. Oncol Rep 2021;46:207

12. Muluhngwi P, Klinge CM. Identification and roles of miR-29b-1-3p and miR29a-3p-regulated and non-regulated lncRNAs in endocrine-sensitive and resistant breast cancer cells. Cancers (Basel) 2021;13:3530

13. Geng A, Luo L, Ren F, Zhang L, Zhou H, Gao X. miR-29a-3p inhibits endometrial cancer cell proliferation, migration and invasion by targeting VEGFA/CD C42/PAK1. BMC Cancer 2021;21:843

14. Zhou W, Li H, Shang S, Liu F. lncRNA KCNQ1OT1 reverses the effect of sevoflurane on hepatocellular carcinoma progression via regulating the miR-29a-3p/CBX3 axis. Braz J Med Biol Res 2021;54:e10213

15. Salih DA, Brunet A. FoxO transcription factors in the maintenance of cellular homeostasis during aging. Curr Opin Cell Biol 2008;20:126-136

16. Gómez-Puerto MC, Verhagen LP, Braat AK, Lam EW, Coffer PJ, Lorenowicz MJ. Activation of autophagy by FOXO3 regulates redox homeostasis during osteogenic differentiation. Autophagy 2016;12:1804-1816

17. Ambrogini E, Almeida M, Martin-Millan M, Paik JH, Depinho RA, Han L, Goellner J, Weinstein RS, Jilka RL, O'Brien CA, Manolagas SC. FoxO-mediated defense against oxidative stress in osteoblasts is indispensable for skeletal homeostasis in mice. Cell Metab 2010;11:136-146

18. Han S, Wang Z, Liu J, Wang HD, Yuan Q. miR-29a-3p-dependent COL3A1 and COL5A1 expression reduction assists sulforaphane to inhibit gastric cancer progression. Biochem Pharmacol 2021;188:114539

19. Liu F, Wang Z, Liu F, Xu J, Liu Q, Yin K, Lan J. MicroRNA-29a-3p enhances dental implant osseointegration of hyperlipidemic rats via suppressing dishevelled 2 and frizzled 4. Cell Biosci 2018;8:55

20. Zeng X, Wang Y, Dong Q, Ma MX, Liu XD. DLX2 activates Wnt1 transcription and mediates Wnt/β-catenin signal to promote osteogenic differentiation of hBMSCs. Gene 2020;744:144564

21. Wu X, Sun W, Tan M. Noncoding RNAs in steroid-induced osteonecrosis of the femoral head. Biomed Res Int 2019; 2019:8140595

22. Chen Y, Zhang W, Yan L, Zheng P, Li J. miR-29a-3p directly targets Smad nuclear interacting protein 1 and inhibits the migration and proliferation of cervical cancer HeLa cells. PeerJ 2020;8:e10148

23. Zhu D, Tian J, Wu X, Li M, Tang X, Rui K, Guo H, Ma J, Xu H, Wang S. G-MDSC-derived exosomes attenuate collagen-induced arthritis by impairing Th1 and Th17 cell responses. Biochim Biophys Acta Mol Basis Dis 2019;1865: 165540

24. Chen D, Gong Y, Xu L, Zhou M, Li J, Song J. Bidirectional regulation of osteogenic differentiation by the FOXO subfamily of Forkhead transcription factors in mammalian MSCs. Cell Prolif 2019;52:e12540

25. Long C, Cen S, Zhong Z, Zhou C, Zhong G. FOXO3 is targeted by miR-223-3p and promotes osteogenic differentiation of bone marrow mesenchymal stem cells by enhancing autophagy. Hum Cell 2021;34:14-27

26. Guérit D, Brondello JM, Chuchana P, Philipot D, Toupet K, Bony C, Jorgensen C, Noël D. FOXO3A regulation by miRNA-29a controls chondrogenic differentiation of mesenchymal stem cells and cartilage formation. Stem Cells Dev 2014;23:1195-1205

27. Fan J, An X, Yang Y, Xu H, Fan L, Deng L, Li T, Weng X, Zhang J, Chunhua Zhao R. MiR-1292 targets FZD4 to regulate senescence and osteogenic differentiation of stem cells in TE/SJ/mesenchymal tissue system via the Wnt/β-catenin pathway. Aging Dis 20184;9:1103-1121

28. Tu X, Delgado-Calle J, Condon KW, Maycas M, Zhang H, Carlesso N, Taketo MM, Burr DB, Plotkin LI, Bellido T. Osteocytes mediate the anabolic actions of canonical Wnt/β-catenin signaling in bone. Proc Natl Acad Sci U S A 2015;112:E478-E486

29. Pei J, Fan L, Nan K, Li J, Shi Z, Dang X, Wang K. Excessive activation of TLR4/NF-κB interactively suppresses the canonical Wnt/β-catenin pathway and induces SANFH in SD rats. Sci Rep 2017;7:11928